HHS Public Access

Author manuscript

Ocul Surf. Author manuscript; available in PMC 2016 July 01.

Published in final edited form as:

Ocul Surf. 2015 July ; 13(3): 226–235. doi:10.1016/j.jtos.2015.02.001.

High-Resolution Fourier-Domain Optical Coherence Tomography as an Adjunctive Tool in the Diagnosis of Corneal and Conjunctival Pathology

Afshan A. Nanji, MD, MPH[1], **Fouad E. Sayyad, MD**[1], **Anat Galor, MD, MSPH**[1,2], **Sander Dubovy, MD**[1,3], and **Carol L Karp, MD**[1]

[1]Department of Ophthalmology, Bascom Palmer Eye Institute, University of Miami, Miami, FL

[2]Miami Veteran Affairs Medical Center, Miami, FL

[3]Florida Lions Ocular Pathology Laboratory, Bascom Palmer Eye Institute, University of Miami, Miami, FL

Abstract

Purpose—To evaluate the use of a commercially-available, high-resolution, spectral-domain optical coherence tomography (HR OCT) device in the diagnosis of corneal and conjunctival pathologies, with a focus on malignant lesions.

Methods—Eighty-two eyes of 71 patients were enrolled in this prospective case series, including 10 normal eyes, 21 with ocular surface squamous neoplasia (OSSN), 24 with a pterygium or pingueculum, 3 with lymphoma, 18 with pigmented conjunctival lesions (nevus, flat melanosis, or melanoma), and 6 with Salzmann's nodular degeneration. Subjects were imaged using photography and HR OCT (RTVue, Optovue, Fremont, CA). When clinically indicated, surgery was performed and histopathologic specimens were correlated with OCT images.

Results—HR OCT was useful in differentiating among various lesions based on optical signs. Specifically, in OSSN, HR OCT findings included epithelial thickening and hyper-reflectivity, whereas pterygia and pinguecula showed a subepithelial mass under thinner epithelium. In lymphoma, a hypo-reflective, homogenous subepithelial mass was observed. Differentiating between pigmented lesions with HR OCT proved more difficult, but certain characteristics could be identified. Eyes with nevi and melanoma both displayed intensely hyper-reflective basal epithelial layers and discrete subepithelial lesions, but could be differentiated by the presence of cysts in nevi and intense shadowing of sublesional tissue in most melanomas.

Conclusion—We found that a commercially-available HR OCT was a useful non-invasive adjunctive tool in the diagnosis of ocular surface lesions.

Correspondence and Reprints: Carol L. Karp, MD, Bascom Palmer Eye Institute, University of Miami Miller School of Medicine, 900 NW 17th Street, Miami, FL 33136, 305-326-6156, ckarp@med.miami.edu.

Conflict of Interest: The authors have no financial interest in any materials or methods described within this article.

Keywords

High-resolution OCT; RTVue; ocular surface lesions; OSSN; melanoma; lymphoma; pterygium

Introduction

Traditional diagnostic methods for ocular surface pathology have included history, clinical examination, impression cytology, and histopathology. In recent years, anterior segment imaging technologies, including ultrasound biomicroscopy[1], confocal microscopy[2–4], and anterior segment optical coherence tomography[1, 5, 6] have also proven useful in the diagnosis and management of these conditions.

Optical coherence tomography (OCT) has been a valuable tool since its introduction to ophthalmology. It has revolutionized the diagnosis and management of retinal conditions and has also been used as an adjunctive technology in the diagnosis of glaucoma[7–9]. The utility of OCT for anterior segment pathology is still being explored but has shown exciting potential in the assessment of the angle[7, 10], in anterior chamber measurements for phakic intraocular lenses[11], and in the evaluation of endothelial graft attachment after endothelial replacement surgery.[12, 13]

OCT has also been used to evaluate anterior segment tumors. A study comparing time-domain (TD) OCT (Visante, Carl Zeiss Meditec, Dublin, CA) versus ultrasound biomicroscopy (UBM) for such tumors concluded that TD OCT may be a useful tool for the evaluation of superficial non-pigmented lesions of the eye, but was of limited general utility compared to UBM because of poorer resolution of pigmented tumors, depth penetration, and image quality.[1] The advent of spectral-domain (SD) OCT, however, has allowed for higher data acquisition rates and axial resolution than could be obtained with the earlier TD OCT[14]. A previously described SD OCT device[15] with ultra-high axial resolution (UHR, defined as <5 μm of resolution) of approximately 3μm (vs. 18 μm with TD OCT) has enabled greater evaluation of lesions of the ocular surface. This UHR OCT has been utilized to differentiate among various corneal pathologies and ocular surface lesions, including ocular surface squamous neoplasia (OSSN), pterygium, and Salzmann's nodular degeneration.[6, 16–18] Unfortunately, the UHR OCT device described in these studies is a custom built device, and not commercially available. However, high-resolution spectral-domain OCTs (HR OCT) with resolution of 5–7 μm, are available, including the RTVue OCT system (Optovue, Fremont, CA), which has an axial resolution of 5 μm and has been approved by the Food and Drug Administration (FDA) as both a retinal and anterior segment imaging device. The instrument has been used in the evaluation of the tear meniscus[19–21] and corneal microarchitecture[22–24], but there is limited information on its utility as an adjunct in the diagnosis and management of ocular surface pathologies.

In this study, we therefore aimed to evaluate the utility of the HR RTVue OCT system in differentiating among various ocular surface pathologies. Specifically, the purpose of our study was to assess whether a commercially-available, high-resolution device could replicate previously published OCT findings obtained with an ultra-high-resolution, but custom-built

device, thus allowing differentiation of various ocular surface tumors and other lesions, with a commercially-available platform.

Methods

This study was approved by the University of Miami Institutional Review Board and was conducted in accordance with the principles of the Declaration of Helsinki. Written informed consent was obtained from all study participants.

Seventy-one patients were recruited to participate in the study; eighty-two eyes of these patients were scanned between November 2011 and October 2012. Inclusion criteria included patients with normal conjunctival and corneal anatomy, those with ocular surface pathologies that were easily identified by clinical examination, and those with ocular surface pathologies in which the diagnosis was clinically ambiguous. Exclusion criteria included the inability to understand the informed consent process or comply with the testing procedures. All patients were evaluated by a corneal specialist (CLK) and underwent clinical photography and HR OCT scanning. An initial clinical diagnosis was made in all cases based on slit-lamp examination.

OCT imaging was performed using a spectral domain OCT (RTVue, Optovue, Fremont, CA software version 6.1.0.4), which has a transverse resolution of 15um, an axial resolution of 5um, a wavelength of 830nm, and which scans at 26,000 A-scans per second. The HR OCT has a corneal lens adapter (cornea anterior module–low magnification [CAM-L]), which is fixed onto the main lens to be able to scan the anterior segment of the eye; it can capture a scan length of up to 10 mm and has a scan depth of 3 mm. The working distance between the lens adapter and cornea is 13 mm on the CAM-L model. The CL-line scan (6–8mm) was used to image all lesions. Using this standard line mode, the location of the line can be seen on the monitor and was initially placed in the middle of the lesion. Scans were then automatically averaged to produce a high quality image; the device automatically averages up to 32 scans.

After several scans were taken, the distance-measuring tool (built into the software) was used to measure the greatest lesional epithelial thickness visualized. A perpendicular line from Bowman’s layer to the tear film was used to measure the epithelium. All patients were scanned and measured by one individual (FES) on the same HR OCT device. All scans and thickness measurements were reviewed by two other authors (CLK and AG). OCT scans were also evaluated in terms of reflectivity of the epithelial and subepithelial components; hyper-reflectivity was defined as increased whiteness compared to tissue of the same location seen in normal subjects, and hypo-reflectivity was defined as increased darkness compared to tissue of the same location seen in normal subjects.

When clinically indicated for either diagnostic or treatment purposes, an incisional or excisional biopsy was performed; biopsy was performed in 33 eyes of 33 individual patients. Lesions with the following clinical diagnoses that were not biopsied included: normal eyes (n=10), OSSN (n=7), pterygia (n=10), pinguecula, (n= 7), conjunctival melanosis consisting of primary acquired melanosis (PAM) (n=2), nevi (n=4), complexion associated melanosis

(CAM) (n=4) and Salzmann's nodular degeneration (n=5). Biopsy specimens were fixed in 10% buffered formalin, dehydrated, and embedded in paraffin blocks. The blocks were sectioned at 5um and were stained with hematoxylin-eosin, periodic acid Schiff, and other indicated stains. These stains were analyzed using a light microscope (Olympus Optical Co., Tokyo, Japan) and were photographed using a digital system.

All statistical analyses were performed using the SPSS 21 (SPSS Inc, Chicago, Illinois, USA) statistical package. Descriptive statistics were used to summarize the ordinal and continuous variables. Student t-tests were used to evaluate differences in mean epithelial thickness between groups. P-values of less than 0.05 were considered significant.

Results

A summary of the patient demographics is shown in Table 1. A summary of the optical signs seen in normal patients and in the various studied lesions is shown in Table 2.

Normal controls

Ten control eyes were included in the study. Figure 1 demonstrates the normal appearance of the cornea, limbus, and conjunctiva on HR OCT. There is a bright white tear film layer overlying the cornea and conjunctiva. The corneal epithelium is dark and thin, while that of the limbus and conjunctiva is thin but mildly hyper-reflective. The normal subepithelial tissue of the cornea is seen in a regular linear pattern, while that of the conjunctiva is less regular and is hyper-reflective, particularly in the most anterior portion. Mean epithelial thickness at the limbus in the ten control eyes was 54.5 μm (standard deviation (SD) 6 μm, range 47–68 μm).

Pterygia/pinguecula

Twenty-four lesions were clinically diagnosed as either a pterygium (Fig 2A; n=17) or pingueculum (n=7). The HR OCT findings of both pterygia (Fig 2B) and pinguecula included mild epithelial hyper-reflectivity (seen in 22 cases) and a normal to slightly thickened epithelium (mean 69 μm, SD 20 μm, range 37–116 μm). The average thickness of the epithelium was greater than in normal controls ($p = 0.005$). Sixteen of the 17 pterygium cases had thick hyper-reflective tissue in the sub-epithelial space, which in many cases was clearly seen between the corneal epithelium and Bowman's layer in the corneal portions of the scan (Fig 2B). All 7 pinguecula cases revealed a dark subepithelial tissue mass close to the limbus. In the 7 pterygium cases in which excisional biopsies were performed, histopathology (Fig 2C) revealed basophilic actinic degeneration located within the substantia propria with an overlying unremarkable epithelium.

Ocular Surface Squamous Neoplasia

Twenty-one OSSN lesions (Fig 3) were included in the study. HR OCT findings at the time of diagnosis (Fig 3B &3C) in all cases included a strongly hyper-reflective epithelium and epithelial thickening. At the thickest measured point, the epithelium measured, on average, 390 μm (SD 247 μm, range 124–1000 μm). The epithelial thickness for OSSN was greater than that seen in all normal controls and in all patients with pterygia or pingueculae. There

was no overlap in the measured epithelial thickness between the OSSN and pterygium/pinguecula groups (p value <0.0005 for epithelial thickness in OSSN eyes compared to control and pterygium/pinguecula eyes). Additionally, when comparing epithelial thickness measurements between OSSN and pinguecula/pterygium, the receiver operating characteristic (ROC) curve showed no overlap between the two groups, with an area under the curve of 100%. Using 120 μm as a cutoff, the sensitivity of HR OCT for differentiating between OSSN and pterygia was 100% and the specificity was 100% in this series.

Besides epithelial thickening, OSSN lesions also demonstrated an abrupt transition between normal and abnormal epithelium, defined as a rapid increase in both brightness and thickness of the epithelium. This finding was visualized in 95% of cases (n=20). In thicker lesions, particularly those with an epithelial thickness greater than 465μm, the inferior border of the epithelium was unable to be delineated in its entirety due to shadowing; this was true in this series in 24% (n=5) of the OSSN lesions. In the 14 OSSN cases with available histopathology, the diagnosis of non-invasive OSSN was confirmed in all cases. The histopathologic findings (Fig 3G) mirrored those of the corresponding HR OCT, with thickened epithelium and an abrupt transition between normal and abnormal epithelium, in all cases.

In OSSN lesions that were resistant to medical treatment (Fig 3E), HR OCT performed after initial treatment demonstrated a persistently thickened epithelium with a retained abrupt transition between the normal to abnormal epithelium. However, for those lesions treated successfully with topical agents (Fig 3F), the post-treatment HR OCT revealed normalization of the corneal and conjunctival epithelial architecture.

HR OCT was instrumental in obtaining a definitive diagnosis in 4 cases of OSSN in which the clinical diagnosis was unclear. Figure 4 shows the left eye of a 49-year-old boat captain who presented to the clinic with a pterygium at the temporal limbus (Fig 4A). On examination, the head of the pterygium appeared somewhat atypical, with a gelatinous appearance. HR OCT was performed (Fig 4B), which revealed a subepithelial hyper-reflective mass as is seen in pterygium. However, overlying the subepithelial mass at the limbus was an area of thickened and highly reflective epithelium, with an abrupt transition from normal to abnormal epithelium, highly suspicious for OSSN. Based on the OCT findings, the lesion was excised with wide margins, and cryotherapy was used. Histopathologic examination (Fig 4C) of the lesion showed faulty epithelial maturational sequencing extending up to full thickness, with subjacent basophilic actinic degeneration, confirming the diagnosis of squamous carcinoma in-situ overlying a pterygium. The HR OCT was also helpful in establishing a diagnosis in 3 other cases in which the architecture of the clinical lesion was ambiguous, in those cases due to a pannus-like appearance or adjacent post-surgical change.

Lymphoma

Three lesions were diagnosed as lymphoma. Slit lamp examination of the lesions revealed salmon-colored conjunctival masses (Fig 5A). The HR OCT findings (Fig 5B) in all cases revealed normal epithelial appearance and thickness (mean 53 μm, SD 12 μm, range 40–63 μm, p=0.72 compared to control eyes). A sub-epithelial mass was identified which was

hypo-reflective and homogenous in all cases. A layer of hyper-reflective, uninvolved substantia propria was noted surrounding the lesion and there was shadowing of the underlying tissue. Extranodal marginal zone lymphoma was confirmed in all cases by histopathology (Fig 5C), flow cytometry and gene rearrangement. All patients underwent treatment with external beam radiation. After radiation, there was resolution of the salmon-colored mass clinically (Fig 5D), and HR OCT (Fig 5E) demonstrated normalization of the conjunctival architecture.

Corneal degeneration

The study included six eyes with the clinical diagnosis of Salzmann's nodular degeneration (Fig 6). HR OCT (Fig 6B) images for these eyes displayed dense, subepithelial, hyper-reflective material just anterior to Bowman's layer with overlying normally reflective, thin epithelium (mean 45 μm, SD 4.6 μm, range 37–49 μm, p=0.005 compared to control eyes). Figure 6 demonstrates a case of a 60-year-old female who was referred by a cornea specialist for possible OSSN in her right eye. Slit lamp examination (Fig 6A) revealed a nasal opalescent lesion. HR OCT (Fig 6B) was consistent with a subepithelial process, such as Salzmann's nodular degeneration but not OSSN. Incisional biopsy was performed for further confirmation based on the patient's request, and histopathology demonstrated mild sub-epithelial fibrosis (Fig 6C), consistent with a corneal degeneration, including Salzmann's nodular degeneration.

Epibulbar Melanocytic Lesions

Eight cases were diagnosed clinically as having melanosis (Figure 7A), either complexion associated melanosis (CAM) or primary acquired melanosis (PAM). HR OCT of flat, melanotic lesions revealed an epithelium of normal thickness (mean 48, SD 13 μm, range 32–64 μm, p=0.75 compared to control eyes). The epithelium in these lesions displayed hyper-reflectivity primarily in the basal epithelium, but with variable extension into the more anterior epithelium (Figure 7B). Epithelial hyper-reflectivity was easiest to appreciate when pigment was present on the cornea because the cornea is innately hypo-reflective and provides greater contrast. No subepithelial mass or cysts were present on HR OCT images of patients with flat melanosis. Histologic correlation was available in two cases of melanosis, one of which confirmed a presumed diagnosis of CAM and the other which confirmed a clinically suspected diagnosis of PAM. Histopathology of PAM demonstrated a correlation between the atypical melanocytes seen within the basal epithelium, with extension into the more superficial layers (Fig 7C), and the hyper-reflectivity of the basal epithelium seen on HR OCT.

Five lesions were clinically diagnosed as nevi. HR OCT for these eyes detected a mildly hyper-reflective epithelium of normal thickness (mean 49 μm, SD 12 μm, range 31–62μm, p=0.29 compared to control eyes). The basal epithelium was strongly hyper-reflective in 4 of the 5 eyes and there was a subepithelial mass of variable reflectivity with mild shadowing noted below the subepithelial mass. By HR OCT, cysts were detected in all cases. Excision was performed in one case, in a patient with a lesion thought clinically to be a nevus but who had recently noted growth of the lesion; histopathology confirmed the clinical diagnosis of a nevus.

Five cases of melanoma were included in the study, 2 with pigment and 3 amelanotic lesions. Similar to the findings with nevi, HR OCT imaging demonstrated a hyper-reflective epithelium with variable thickening among the lesions (mean 68 μm, SD 25 μm, range 37–99 μm, p=0.30 compared to control eyes). There was also intense hyper-reflectively of the basal epithelium and a hyper-reflective subepithelial mass (Fig 8B). Significant shadowing was observed secondary to the pigmented subepithelial mass, which in many cases obscured the posterior portion of the lesion and the underlying tissue. In contrast to the findings with nevi, no cysts were seen in the 5 melanoma cases. Histopathology was available and confirmed the diagnosis of melanoma for all cases.

For all 3 cases of amelanotic melanoma (Figure 8A), the diagnosis was unclear by clinical examination and the patients were referred to the clinic for treatment of probable OSSN. HR OCT of the lesions was performed in each case (Fig 8B), which revealed mild epithelial thickening, but also a large hyper-reflective mass with shadowing below the lesion. The HR OCT finding of a subepithelial mass was not consistent with OSSN, and the lesions were therefore excised with wide margins and cryotherapy, instead of attempting medical treatment. Histopathologic examination (Fig 8C) from the excision disclosed nests of atypical melanocytes in the epithelium and substantia propria, consistent with melanoma.

Reproducibility of findings

All patients had their OCTs reviewed at the time of the clinical examination by one author of the current study (CLK). In addition, the OCT images were evaluated by two other authors (AG and AN) who were comfortable reading OCTs but who were unaware of the clinical diagnosis, in order to evaluate the reproducibility of the above results. They were able to correctly identify whether the imaged lesions were or were not OSSN in 88.5% and 93.6% of cases, respectively.

Discussion

In this study, we found that the RTVue, a commercially available, HR OCT device, was able to demonstrate many of the optical signs of various ocular surface pathologies that we have previously described using a custom-built machine[6, 16–18]. Additionally, we were able to use the HR OCT device to differentiate between lesions that were clinically ambiguous, allowing a decision to be made for appropriate care of patients.

The RTVue HR OCT has several particular software functions that are useful in the evaluation of ocular surface lesions. First, a real time image of the ocular surface is provided, allowing documentation of the location of the scan being performed. Additionally, the device allows for direct measurements on the scan itself, permits side-by-side comparison with prior scans, and allows the user to invert the image to a negative image, which in some cases is useful in outlining the edges of the lesion.

The HR OCT was particularly useful in the diagnosis of OSSN and in differentiating OSSN from mimicker lesions such as amelanotic melanoma and corneal fibrosis. Images obtained on the RTVue device were able to demonstrate the morphologic features of OSSN, such as a thickened epithelium and an abrupt transition from normal to abnormal epithelium. In a

variety of cases, the presence or absence of these HR OCT findings promoted an appropriate course of treatment for patients which differed from that determined from clinical exam alone, such as in three patients with amelanotic melanoma and one case of a patient with an OSSN within a pterygium. In a recent study by Adler *et al*.[25], approximately 50% of the members of the Ocular Microbiology and Immunology Group who responded to a mail survey, reported that they did not always biopsy suspected OSSN prior to initiation of topical agents. Imaging can therefore be useful as a non-invasive approach to confirm the diagnosis of OSSN, differentiating it from amelanotic melanoma, corneal scarring or pannus, or other mimicker lesions.

In addition to diagnosis, the HR OCT was also found to be useful in monitoring for OSSN resolution during medical treatment. In several of the cases of OSSN, HR OCT images obtained during treatment were able to detect subtle residual epithelial thickening not seen on clinical examination, thus avoiding possible premature termination of treatment. Monitoring resolution with the HR OCT was particularly useful in cases of concurrent ocular surface pathology, such as limbal stem cell deficiency, in which subtle lesions or residual neoplasia were difficult to detect in the setting of adjacent pannus or scarring. We suspect that residual microscopic disease is a cause of tumor recurrence and that perhaps continued treatment until normalization of the OCT may decrease recurrence, although this hypothesis requires further evaluation.

Limitations to OCT technology, however, do exist. First, OCT cannot characterize cellular details, and therefore, at this point, flat melanotic lesions cannot be differentiated in terms of the presence of atypia. Additionally, the averaging of the individual scans may normalize existing pathology, such as small cysts within lesions, making subtle pathology more difficult to detect. Of note, individual scans can be reviewed in such cases. With thicker lesions, the OCT image also often demonstrates shadowing, thus obscuring the inferior boundary of the lesion, and likely, obscuring the ability to detect invasion into the sclera. To date, it is not known whether HR OCT is able to distinguish between patients with invasive squamous cell carcinoma (SCC) versus squamous intraepithelial lesions; none of the patients in the current study who underwent biopsy had SCC. This limitation is relevant because although topical treatment can be used for SCC, these patients may require more prolonged courses of medication for resolution.[26] Lastly, although limbal lesions are easily scanned with OCT, those in the fornix and caruncle are more challenging.

In this study, 3 independent reviewers evaluated the OCT images and arrived at similar conclusions. While encouraging, we cannot definitively comment on how well other clinicians, less experienced with reading HR-OCT, would fare and are currently performing further studies to explore this question. Another consideration is that only a select number of cases were included in each pathology group and not all had pathologic confirmation, which also reduces the study's generalizability. However, in those cases for which tissue was obtained, we did find excellent correlation between the OCT and histology. A larger study, with more cases and with more diagnoses included, such as infections, autoimmune disorders, and allergy, will help validate and expand our initial findings.

While the possibility of using the epithelial thickness as a sensitive method of diagnosis of OSSN is exciting and tempting, it is important to keep in mind that the optimal number for each device is not yet known. Using the RTVue we found that the epithelial thickness of all OSSN lesions was greater than 120 um and the thickness of all pterygia was less than 120 um. In a previous study[16] using a custom built ultra high resolution OCT device, we found that a thickness of 142 um maximized the sensitivity and specificity with regards to OSSN and pterygium differentiation. As such, it is important to emphasize that no number can be definitively used to diagnose OSSN and that all data should be considered within the clinical scenario. The HR OCT can, however, be a helpful part of diagnosis of OSSN, especially in ambiguous cases.

In summary, we were able to utilize HR OCT to determine the etiology of and to differentiate between multiple ocular surface lesions, including OSSN, pterygium, nevi, and melanoma, as well as to evaluate resolution of disease after treatment. Of these lesions, the technology was most useful in differentiating OSSN from other corneal and conjunctival pathologies and in several cases was used to guide appropriate management. The technology was less useful in evaluating pigmented lesions, and clinicians should continue to obtain pathology in cases in which interpretation of OCT findings are challenging.

This pilot study is important in that we utilized a commercially-available device to assist with the diagnosis and management of ocular surface pathologies. While the technology cannot substitute for either clinical evaluation or histopathologic diagnosis, it may be used as an important adjunct in determining the diagnosis in difficult ocular surface cases and in assessing disease resolution. We therefore see this instrument as a promising, useful, and non-invasive addition to the current toolbox of anterior segment imaging technologies.

Acknowledgments

Financial Support: Supported in part by NIH Center Core Grant P30EY014801, Research to Prevent Blindness Unrestricted Grant, Department of Defense (DOD-Grant#W81XWH-09-1-0675), The Ronald and Alicia Lepke Grant, The Lee and Claire Hager Grant, The Richard Azar Family Grant and The Jimmy and Gaye Bryan Grant (all institutional grants).

References

1. Bianciotto C, Shields CL, Guzman JM, et al. Assessment of anterior segment tumors with ultrasound biomicroscopy versus anterior segment optical coherence tomography in 200 cases. Ophthalmology. 2011; 118:1297–302. [PubMed: 21377736]
2. Xu Y, Zhou Z, Xu Y, et al. The clinical value of in vivo confocal microscopy for diagnosis of ocular surface squamous neoplasia. Eye (Lond). 2012; 26:781–7. [PubMed: 22402703]
3. Parrozzani R, Lazzarini D, Dario A, Midena E. In vivo confocal microscopy of ocular surface squamous neoplasia. Eye (Lond). 2011; 25:455–60. [PubMed: 21311574]
4. Messmer EM, Mackert MJ, Zapp DM, Kampik A. In vivo confocal microscopy of pigmented conjunctival tumors. Graefes Arch Clin Exp Ophthalmol. 2006; 244:1437–45. [PubMed: 16598465]
5. Shields CL, Belinsky I, Romanelli-Gobbi M, et al. Anterior segment optical coherence tomography of conjunctival nevus. Ophthalmology. 2011; 118:915–9. [PubMed: 21146221]
6. Shousha MA, Karp CL, Canto AP, et al. Diagnosis of ocular surface lesions using ultra-high-resolution optical coherence tomography. Ophthalmology. 2013; 120:883–91. [PubMed: 23347984]

7. Radhakrishnan S, See J, Smith SD, et al. Reproducibility of anterior chamber angle measurements obtained with anterior segment optical coherence tomography. Invest Ophthalmol Vis Sci. 2007; 48:3683–8. [PubMed: 17652739]
8. Kanamori A, Nakamura M, Escano MF, et al. Evaluation of the glaucomatous damage on retinal nerve fiber layer thickness measured by optical coherence tomography. Am J Ophthalmol. 2003; 135:513–20. [PubMed: 12654369]
9. Pieroth L, Schuman JS, Hertzmark E, et al. Evaluation of focal defects of the nerve fiber layer using optical coherence tomography. Ophthalmology. 1999; 106:570–9. [PubMed: 10080216]
10. Sakata LM, Lavanya R, Friedman DS, et al. Comparison of gonioscopy and anterior segment ocular coherence tomography in detecting angle closure in different quadrants of the anterior chamber angle. Ophthalmology. 2008; 115:769–74. [PubMed: 17916377]
11. Goldsmith JA, Li Y, Chalita MR, et al. Anterior chamber width measurement by high-speed optical coherence tomography. Ophthalmology. 2005; 112:238–44. [PubMed: 15691557]
12. Kymionis GD, Ide T, Donaldson K, Yoo SH. Diagnosis of Donor Graft Partial Dislocation Behind the Iris After DSAEK with Anterior Segment OCT. Ophthalmic Surg Lasers Imaging. 2010:1–2.
13. Yeh RY, Quilendrino R, Musa FU, et al. Predictive value of optical coherence tomography in graft attachment after Descemet's membrane endothelial keratoplasty. Ophthalmology. 2013; 120:240–5. [PubMed: 23149125]
14. Kiernan DF, Mieler WF, Hariprasad SM. Spectral-domain optical coherence tomography: a comparison of modern high-resolution retinal imaging systems. Am J Ophthalmol. 2010; 149:18–31. [PubMed: 20103039]
15. Shousha MA, Perez VL, Wang J, et al. Use of ultra-high-resolution optical coherence tomography to detect in vivo characteristics of Descemet's membrane in Fuchs' dystrophy. Ophthalmology. 2010; 117:1220–7. [PubMed: 20163865]
16. Kieval JZ, Karp CL, Abou Shousha M, et al. Ultra-high resolution optical coherence tomography for differentiation of ocular surface squamous neoplasia and pterygia. Ophthalmology. 2012; 119:481–6. [PubMed: 22154538]
17. Shousha MA, Karp CL, Perez VL, et al. Diagnosis and management of conjunctival and corneal intraepithelial neoplasia using ultra high-resolution optical coherence tomography. Ophthalmology. 2011; 118:1531–7. [PubMed: 21507486]
18. Vajzovic LM, Karp CL, Haft P, et al. Ultra high-resolution anterior segment optical coherence tomography in the evaluation of anterior corneal dystrophies and degenerations. Ophthalmology. 2011; 118:1291–6. [PubMed: 21420175]
19. Qiu X, Gong L, Sun X, Jin H. Age-related variations of human tear meniscus and diagnosis of dry eye with Fourier-domain anterior segment optical coherence tomography. Cornea. 2011; 30:543–9. [PubMed: 21107246]
20. Bujak MC, Yiu S, Zhang X, et al. Serial measurement of tear meniscus by FD-OCT after instillation of artificial tears in patients with dry eyes. Ophthalmic Surg Lasers Imaging. 2011; 42:308–13. [PubMed: 21800803]
21. Park DI, Shin HM, Lee SY, Lew H. Tear production and drainage after botulinum toxin A injection in patients with essential blepharospasm. Acta Ophthalmol. 2013; 91:e108–12. [PubMed: 23425111]
22. Tay E, Li X, Chan C, et al. Refractive lenticule extraction flap and stromal bed morphology assessment with anterior segment optical coherence tomography. J Cataract Refract Surg. 2012; 38:1544–51. [PubMed: 22906441]
23. Ahn H, Kim JK, Kim CK, et al. Comparison of laser in situ keratomileusis flaps created by 3 femtosecond lasers and a microkeratome. J Cataract Refract Surg. 2011; 37:349–57. [PubMed: 21241920]
24. Rocha KM, Perez-Straziota CE, Stulting RD, Randleman JB. SD-OCT analysis of regional epithelial thickness profiles in keratoconus, postoperative corneal ectasia, and normal eyes. J Refract Surg. 2013; 29:173–9. [PubMed: 23446013]
25. Adler E, Turner JR, Stone DU. Ocular surface squamous neoplasia: a survey of changes in the standard of care from 2003 to 2012. Cornea. 2013; 32:1558–61. [PubMed: 24145630]

26. Shah SU, Kaliki S, Kim HJ, et al. Topical interferon alfa-2b for management of ocular surface squamous neoplasia in 23 cases: outcomes based on American Joint Committee on Cancer classification. Arch Ophthalmol. 2012; 130:159–64. [PubMed: 22332208]

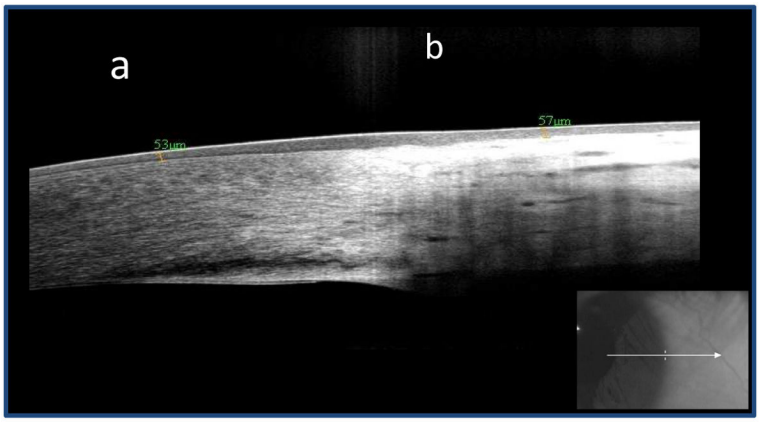

Figure 1.

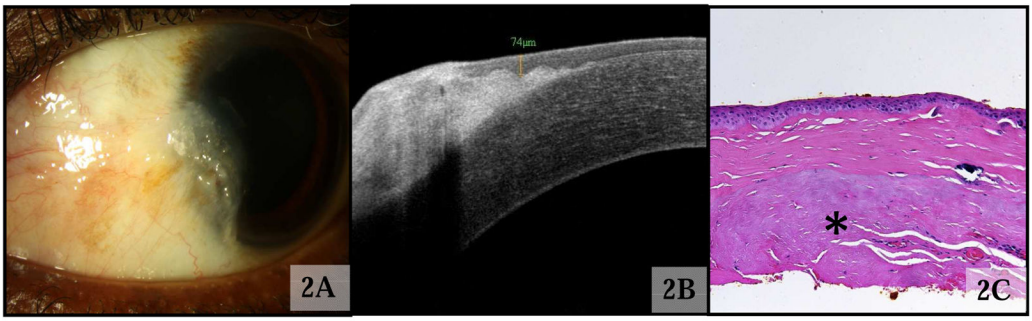

Figure 2.

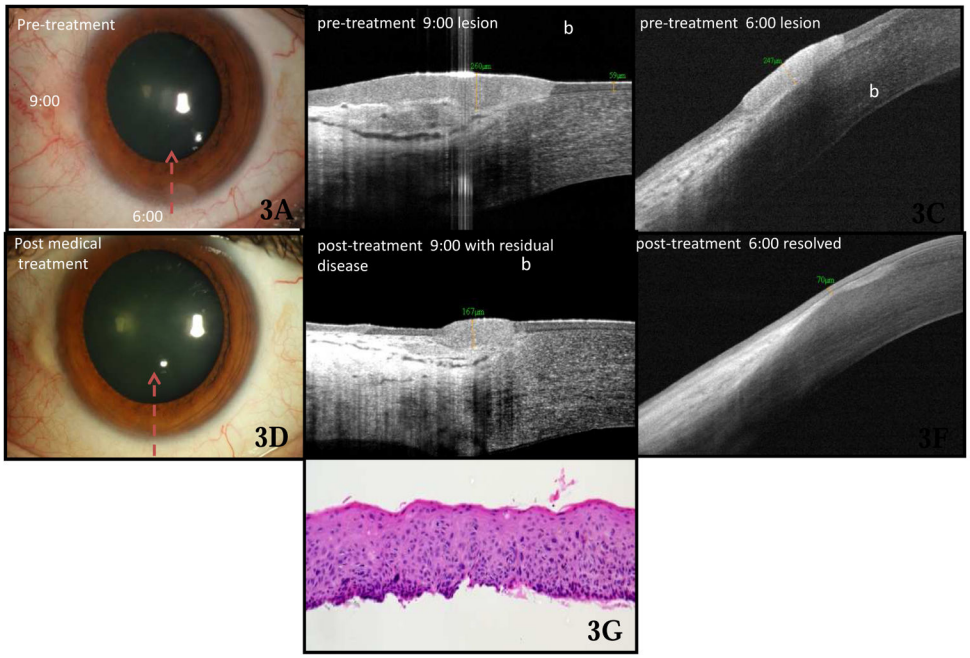

Figure 3.

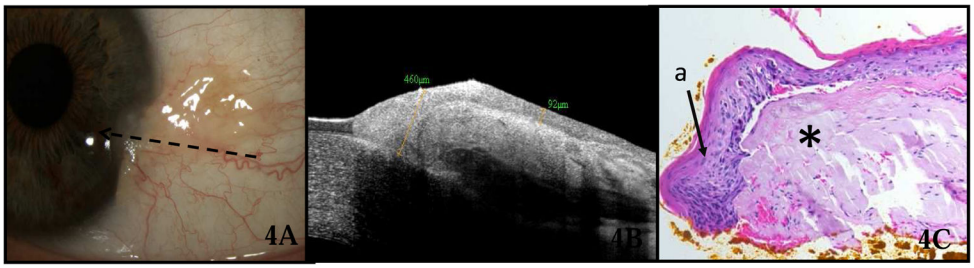

Figure 4.

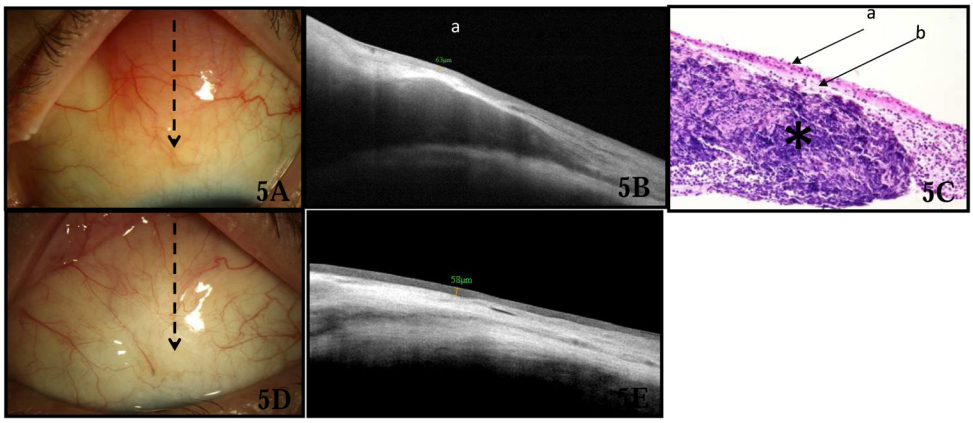

Figure 5.

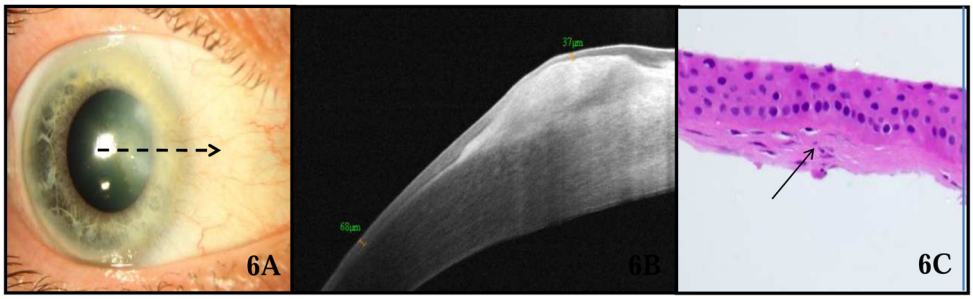

Figure 6.

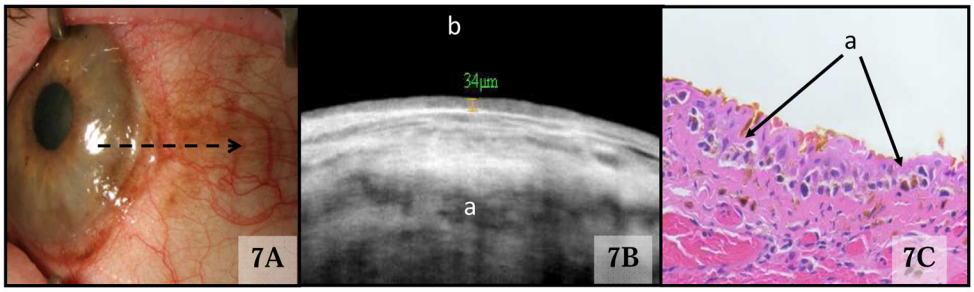

Figure 7.

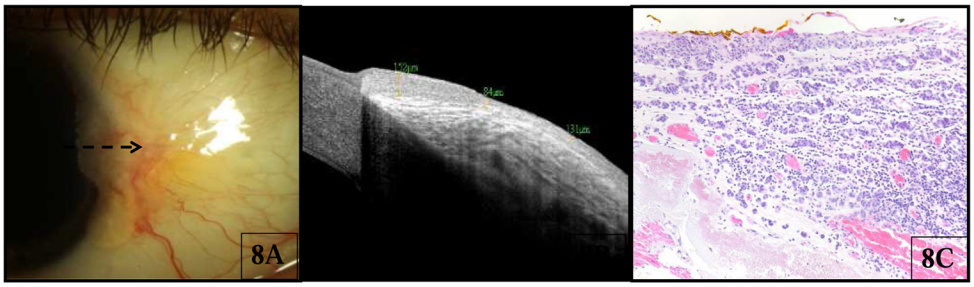

Figure 8.

Table 1

Patient Demographics

Diagnosis (n*)	Mean age (range)	Gender, male n (%)	Race, white n (%) black n (%) other/unknown n (%)	Hispanic ethnicity, n (%)
Normal (6)	41 (25–63)	2 (33%)	5 (83%) 0 (0%) 1 (17%)	4 (67%)
OSSN (21)	64 (41–87)	19 (90%)	19 (90%) 1 (5%) 1 (5%)	11 (52%)
Pinguecula (6)	61 (32–79)	4 (67%)	3 (50%) 1 (17%) 2 (33%)	3 (50%)
Pterygium (17)	51 (39–69)	12 (71%)	14 (82%) 2 (12%) 1 (6%)	8 (47%)
Lymphoma (3)	60 (54–65)	1 (33%)	2 (67%) 0 (0%) 1 (33%)	0 (0%)
Salzmann nodular degeneration (5)	64 (55–76)	2 (40%)	5 (100%) 0 (0%) 0 (0%)	2 (40%)
Flat melanosis (7)	65 (19–82)	4 (57%)	4 (57%) 0 (0%) 3 (43%)	1 (14%)
Nevus (5)	47 (19–75)	3 (60%)	3 (60%) 0 (0%) 2 (40%)	2 (40%)
Melanoma (5)	70 (48–90)	3 (60%)	4 (80%) 0 (0%) 1 (20%)	1 (20%)

*n=number of patients in group; OSSN= ocular surface squamous neoplasia

Table 2

Optical signs of ocular surface lesions

Lesion	Epithelial Layer		Subepithelial layer
	Thickness	Reflectivity	
Normal	Thin epithelium (about 45–70um)	Dark corneal epithelium; mild hyper-reflectivity over limbus and conjunctiva	No masses, no shadowing, anterior portion of conjunctival epithelium hyperreflective
OSSN	Severely thickened; inferior border of lesion may be partially obscured by shadowing in very thick lesions	Strongly hyper-reflective, usually with abrupt transition from normal to abnormal	Not involved in CCIN; unable to comment for SCC (none in current study)
Pingueculum	Normal to slightly thickened epithelium	Mildly hyper-reflective	Dark subepithelial tissue mass near limbus
Pterygium	Normal to slightly thickened epithelium	Mildly hyper-reflective	Highly hyper-reflective subepithelial lesion; hyper-reflective layer seen between Bowman's and corneal epithelium in corneal scans
Lymphoma	Normal thickness	Normal	Hypo-reflective and homogenous subepithelial mass; surrounding hyper-reflective layer of uninvolved tissue and shadowing of underlying tissue
Salzmann's nodular degeneration	Thin epithelium, usually thinner than normal	Normal	Dense, subepithelial, hyper-reflective material just anterior to Bowman's layer
Flat melanosis	Normal thickness	Hyper-reflectivity of the basal epithelium ± patchy hyper-reflectivity within epithelium	No involvement
Nevi	Normal thickness	Mildly hyper-reflective but often with strong reflectivity of basal epithelium	Subepithelial mass with mild shadowing of the underlying tissue; cysts often seen
Melanoma	Normal thickness to somewhat thickened epithelium	Mildly hyper-reflective but often with strong reflectivity of basal epithelium	Hyper-reflective subepithelial mass with obscuration of the underlying tissue (and in some, the posterior portion of the lesion) due to shadowing; rarely cysts.

OSSN=ocular surface squamous neoplasia; CCIN=corneal and conjunctival intraepithelial neoplasia; SCC=squamous cell carcinoma